land

MDPI

Article

Quantitative Geodiversity Assessment and Functional Zoning of Longhushan UNESCO Global Geopark of Southeast China

Haihong Liu [1], Liuqin Chen [1,*], Young Ng [2] and Boshuo Li [1]

[1] School of Earth and Planetary Sciences, East China University of Technology, Nanchang 330013, China; liu-haihong@ecut.edu.cn (H.L.); liboshuo0533@ecut.edu.cn (B.L.)
[2] School of Geography, Planning, and Spatial Sciences, University of Tasmania, Hobart, TAS 7001, Australia; young.ng@utas.edu.au
* Correspondence: chenliuqin@ecut.edu.cn

Abstract

Longhushan UNESCO Global Geopark (UGGp) of Southeast China is characterized by a well-developed red-bed rock landscape with outstanding geoheritage value and diverse geomorphological features. However, a systematic quantitative assessment of its geodiversity has yet to be conducted, constraining spatially explicit strategies for geoheritage conservation and sustainable management. This study developed an eight-indicator assessment framework integrating geology, geomorphology, hydrology and pedology and integrated field survey data with GIS-based spatial analysis. Principal component analysis (PCA) was used to derive objective indicator weights, and a geodiversity index (GI) was calculated for 1 km × 1 km grid cells and classified into five levels using natural breaks. Very high and high GI areas account for 22.30% of the total area and are concentrated mainly in Xianshuiyan, Xiangshan, Guifeng, and Yingtianshan, whereas low and very low GI areas together account for 50.22% and are distributed mainly in the central and northwestern parts and peripheral plains of the geopark; the remaining 27.48% falls within the moderate class, transitional between the two patterns. High GI areas broadly coincide with representative rock landforms and are associated primarily with topographic differentiation, lithological diversity, and fractures. Based on the GI pattern, Longhushan UGGp is divided into core conservation and utilization zone, key conservation and utilization zone, and ecological conservation buffer zone. This first quantitative geodiversity assessment of Longhushan UGGp provides a spatial basis for geoconservation, geotourism planning, and sustainable management of comparable red-bed conglomerate terrains in Southeast China.

Keywords: geodiversity; quantitative assessment; geoheritage; rock landscape; Longhushan UNESCO Global Geopark

Check for updates

Academic Editors: Ana Vovk, Laura Melelli and Borut Stojilković

Received: 19 August 2026
Revised: 9 September 2026
Accepted: 14 September 2026
Published: 18 September 2026

Copyright: © 2026 by the authors. Licensee MDPI, Basel, Switzerland. This article is an open access article distributed under the terms and conditions of the Creative Commons Attribution (CC BY) license.

1. Introduction

In recent decades, geodiversity research has developed rapidly, particularly in quantitative assessment and spatial mapping [1–3]. Quantitative geodiversity assessment is increasingly used to identify conservation priorities [4] and support geotourism development [5], geopark management [6], geoeducation [7], and sustainable land planning [8–10]. By transforming various geological, geomorphological, hydrological, and soil information into spatially explicit indices, such assessments provide an objective basis for recognizing areas of high geodiversity and formulating targeted conservation and management strategies [2,11]. In protected areas such as UNESCO Global Geoparks, however, the spatial

expression and conservation condition of geological and geomorphological features may also be influenced by human modification of the territory [8,12]. Previous studies have linked geodiversity assessment with sustainable land planning and demonstrated spatial relationships between geodiversity and land-use patterns [9,13].

Geodiversity assessment has generally been conducted through either qualitative or quantitative approaches [14,15]. Among them, qualitative research typically employs methods such as literature review, field surveys, and questionnaire interviews to compile geoheritage inventories and maps [16]. These methods are mainly used for the description of characteristics, classification, and values of geodiversity. In contrast, quantitative assessment methods are typically based on a set of parameters and indicators, utilizing geographic information technology and quantitative evaluation models to present the richness and spatial distribution of geodiversity in a more objective manner. In quantitative assessment, the most commonly used approach is the geodiversity index (GI) method. The GI was first proposed as a qualitative model by Serrano & Ruiz-Flaño [1] and was later developed into a GIS-based quantitative assessment model by Pereira et al. [11]. It has been widely applied in studies worldwide and further modified and upgraded in some studies [17,18]. Globally, a large number of quantitative geodiversity assessments have been conducted at various spatial scales. At the national scale, studies include those conducted in Brazil [19], Italy [20], Argentina [21], and Iran [22]. Regional-scale research has also been performed. Carrión-Mero et al. [23] assessed the regional-scale geodiversity of Ecuador and proposed future strategies for geoconservation. Gakou et al. [24] investigated the relationship between geodiversity and biodiversity in southern France. A growing body of research has also focused on geoparks. A framework for assessing local-scale geodiversity for various landforms in the Rokua UGGp of Finland was presented by Tukiainen et al. [25]. Zhang et al. [26] quantitatively assessed the geodiversity of Danxiashan UGGp using map algebra. Some studies have integrated geodiversity assessments into territorial spatial planning to guide regional functional zoning. For instance, a nationwide geodiversity assessment in Ecuador successfully identified key areas of national conservation priority [23]. Similarly, at Cangshan UGGp, a quantitative evaluation based on spatial density indicators established a reproducible and verifiable technical framework for delineating conservation boundaries and formulating management strategies [27]. Collectively, these studies have advanced both the theoretical development and practical application of geodiversity assessment, providing valuable methodological insights for geopark conservation and management.

Red-bed rock landscapes developed on terrestrial conglomerate-dominated successions of the Cretaceous age are distinctive in Southeast China and are distinguished by the development of reddish escarpments with striking natural beauty [28,29]. Among these, China Danxia stands as the most famous example and a serial World Natural Heritage property. Longhushan, a prominent example, is renowned for its well-developed rock landscape featuring sub-rounded summits and prominent red cliffs and also for preserving rich cultural relics. Recognizing its significant geoheritage and cultural values, Longhushan was successively designated as a National Geopark, a National 5A-level Tourist Attraction, a Global Geopark, and a World Heritage Site. In recent years, much progress has been made in understanding the tectonic evolution [30], spatial distribution [31], geomorphic characteristics [32], and formation mechanisms [33,34] of rock landscapes in Longhushan UGGp. However, the geodiversity of Longhushan UGGp has not yet been quantified, and its spatial differentiation remains insufficiently understood, hindering effective conservation and management. This study constructs a geodiversity assessment system for Longhushan UGGp based on eight indicators, with PCA used to derive objective factor weights and GIS-based spatial analysis and weighted overlay applied to calculate the GI. The resulting pattern is used to delineate functional zones for differentiated conservation

and utilization, providing a reference for geoheritage management, geoconservation, and geotourism development in Longhushan and comparable protected areas.

2. Study Area

2.1. Geological Settings

The Xinjiang Basin in northeastern Jiangxi Province is one of the terrestrial fault basins formed during the late Mesozoic era in South China. It is located on the southeastern edge of the Eurasian Plate, in the eastern segment of the suture zone between the Yangtze and Cathaysian plates (Figure 1a) [35]. Longhushan UGGp is situated on the southern margin of the Xinjiang Basin, covers an area of 996.63 km^2, and comprises three scenic areas of Longhushan, Xiangshan, and Guifeng from west to east (Figure 1b). It is bordered by the Xin River Valley to the north and the Wuyi Mountains to the south. It has a subtropical humid monsoon climate, with an average annual temperature of 18 °C and an average annual precipitation of 1878 mm. The Xin River runs from east to west through the Guifeng and Xiangshan scenic areas. The Luxi River, a tributary of the Xin River, flows from southeast to northwest through the Longhushan scenic area.

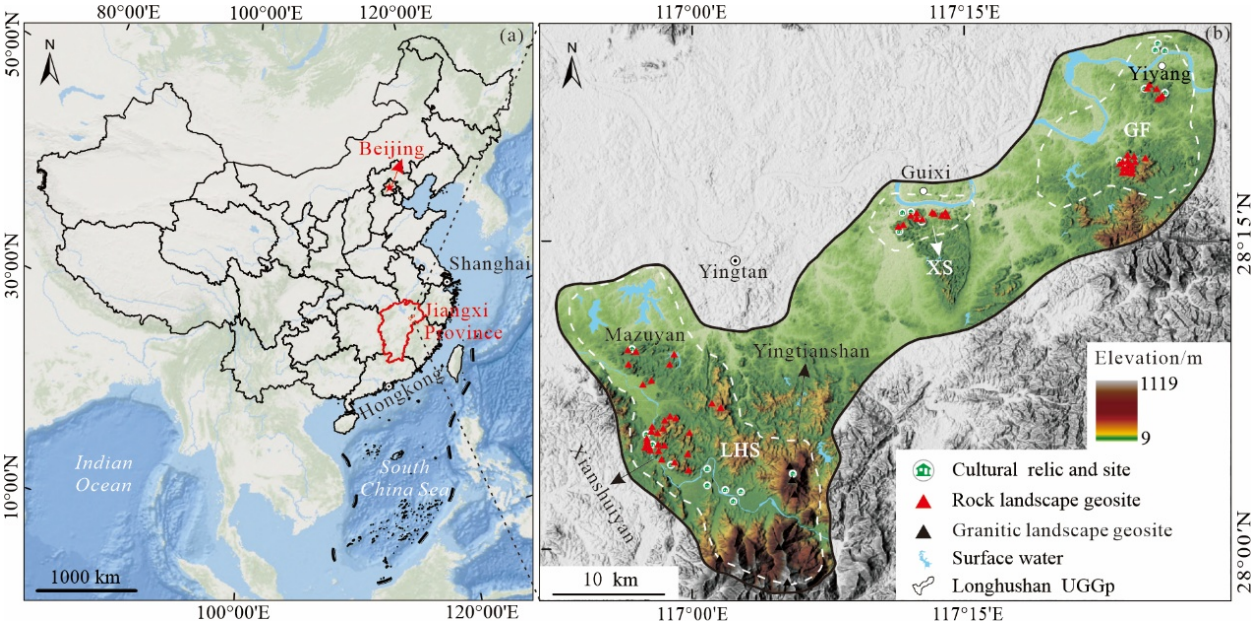


Figure 1. Location and topography of Longhushan UGGp. (**a**) Location of Longhushan UGGp in southeastern China, with Jiangxi Province outlined in red. (**b**) Digital elevation model (DEM) of Longhushan UGGp, showing the distribution of rock landscape geosites, granitic landscape geosites, cultural relics, and surface water. The white dashed lines denote the boundaries of the Longhushan (LHS), Xiangshan (XS), and Guifeng (GF) scenic areas.

The geopark is dominated by terrestrial clastic rocks of Late Cretaceous age, whereas metamorphic rocks of the Neoproterozoic and granitic volcanic-intrusive complexes of the Jurassic outcrop sporadically in the east and southwest (Figure 2). The Late Cretaceous strata are divided into the Ganzhou and Guifeng groups. The Guifeng Group is generally coarse-grained and is subdivided into the Hekou, Tangbian, and Lianhe formations in ascending order [36]. The bedrock underlying the valuable geoheritage of the landscape is composed of the Hekou and Tangbian formations [30,34]. The Hekou Formation is dominated by conglomerates with minor amounts of sandstones. These rocks are cemented primarily by ferric oxides and calcite minerals. In contrast, the Tangbian Formation is mainly composed of aeolian sandstones and is dominated by calcite cements [37].

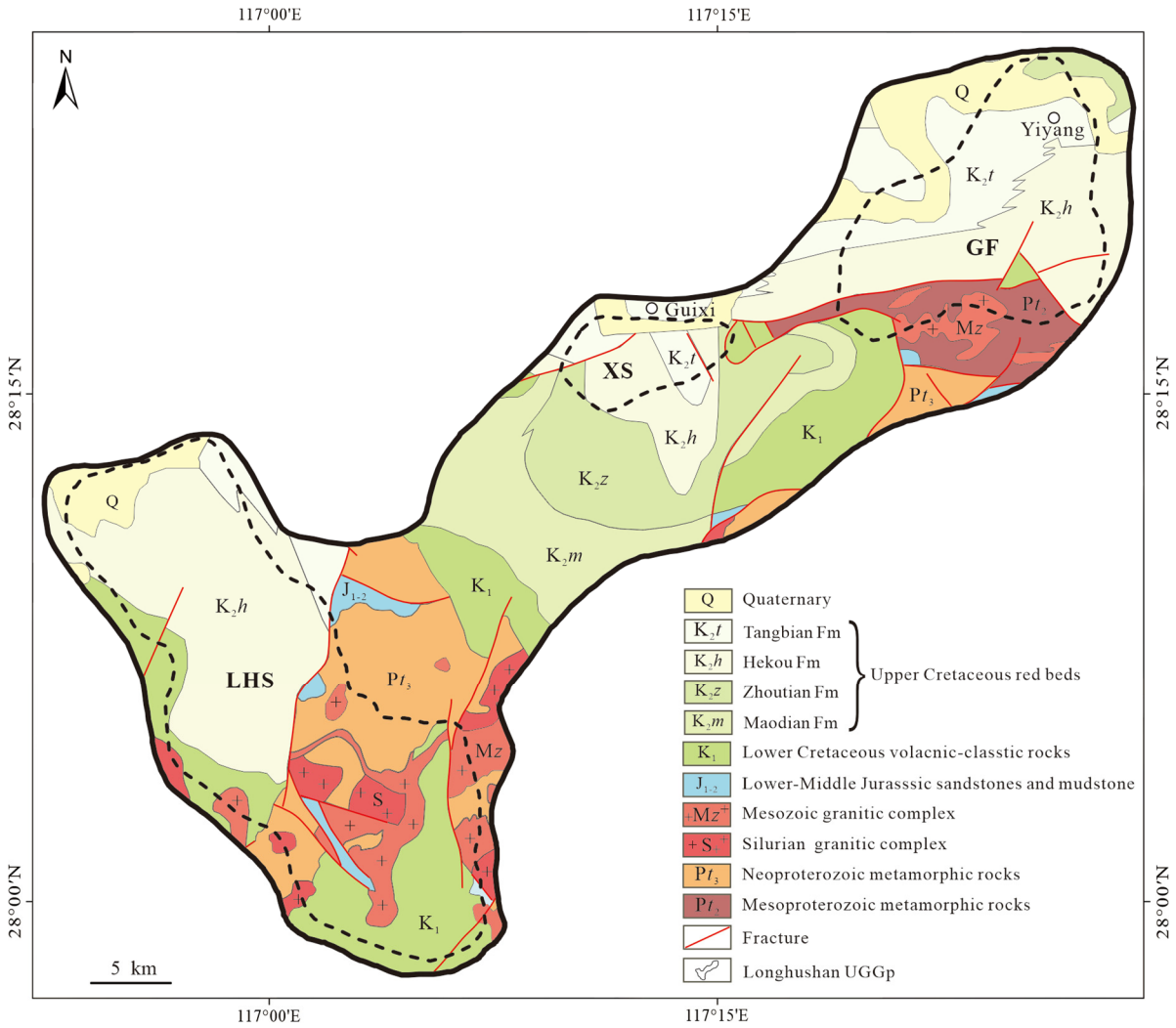


Figure 2. Geological map of Longhushan UGGp [36]. Geological map of Longhushan UGGp, showing the stratigraphic units, igneous rocks, unconformities, and tectonic fractures.

Within the Xinjiang Basin, the clastic rock tableland has been intensely dissected by three sets of fractures trending in NE, NW, and E-W directions [31]. Influenced by regional boundary fault activities, the crust on the north and south margins of the Xinjiang Basin undergoes differential uplift and subsidence, leading to systematic variations in the attitude of the red beds, with the dip angle of strata increasing from the basin center to the margins [38]. The rock formations were dissected by conjugate joints into blocks, producing a network-like distribution of landforms [32].

2.2. Geomorphological Settings—Landscape and Landforms

Longhushan UGGp features scattered blocks and sparse peak forests, with gentle terrain relief and a maximum relative elevation of approximately 476 m. According to morphological characteristics, the erosional landscape in Longhushan UGGp can be classified into monomorphic types and compound types. Monomorphic landform types include peaks, cliffs, walls, towers, pillars, domes, ravines, canyons, and cavernous weathering features. The compound types are characterized by the coexistence of peak clusters, peak forests, and residual hills [38].

The geomorphological characteristics also vary spatially within the geopark. The Xianshuiyan area of the Longhushan scenic area is typified by dispersed peak forests in broad valleys (Figure 3a). These landforms are characterized by relatively isolated

rock masses separated by fluvial corridors and low-lying terrain. The Guifeng scenic area is characterized by the coexistence of isolated peaks and residual hills, producing a more fragmented landscape pattern. In addition, the Yingtianshan area is underlain mainly by Jurassic granitic rocks and is characterized by great topographic relief, offering impressive waterfall scenery (Figure 3g) when rainfall is plentiful during the spring and summer seasons. These spatial differences provide the geomorphological background for the distribution of representative geosites described below.



Figure 3. Typical rock landscape and landforms in Longhushan UGGp. (**a**) Landscape of red hills and the Luxi River at Xianshuiyan. (**b**) Sandie (three stacked) Turtles showing densely developed vertical joints at Guifeng. (**c**) Bedding cavities along cliff faces at Xianshuiyan. (**d**) Jinqiang Pillar in Longhushan. (**e**) Wall and arcade at Xiangbi Hill. (**f**) A large arch (Xianqiao, Immortal Bridge) developed in aeolian sandstone of the Tangbian Formation at Xiangshan. (**g**) Waterfall along the granite ravine. (**h**) Zhengyi Taoist Temple. (**i**) Xiangshan Academy.

2.3. Geosites

The geosites of Longhushan UGGp are dominated by erosional landforms developed in the Late Cretaceous red beds, except in the Yingtianshan area, which is underlain by Jurassic granitic intrusions. Representative geosites of the three scenic areas are presented in Figure 1b and briefly described below. These geosites are described to characterize the principal geoheritage features of Longhushan UGGp and to support the interpretation of the geodiversity assessment results; they were not included as indicators in the calculation of the geodiversity index (GI).

In the Longhushan scenic area, Paiya Peak is a representative peak cluster geosite, which extends approximately 2 km from north to south and reaches a maximum height of 270 m. In addition, a number of isolated pillars and collapse remnants are distributed throughout this area. Jinqiang Pillar (Figure 3d) and Fairy Rock are representative pillar landforms that have become popular tourist attractions. Xiangbi (Elephant Trunk) Hill is a collapse residual characterized by a natural rock arcade (Figure 3e).

The Xiangshan scenic area is distinguished by the presence of Xianqiao (Immortal Bridge), a large natural arch developed within the aeolian sandstones of the Tangbian Formation (Figure 3f). It measures 23.85 m in length, 6.43 m in width, and 9.44 m in height.

The Guifeng scenic area is characterized by the coexistence of isolated peaks and residual hills. Among these, Sandiegui (Three Stacked Turtles) is the most representative, exhibiting densely developed vertical joints that have partitioned the rock mass into columnar blocks (Figure 3b).

2.4. Cultural Landscape

Among the serial property sites of World Heritage China Danxia, Longhushan possesses the most profound and distinctive Chinese traditional culture. Over 200 hanging coffins of the ancient Yue people are preserved within bedding cavities in the Xianshuiyan, Baojia Peak, and Luosiling areas (Figure 3c), which were collectively designated as Major Historical and Cultural Sites Protected at the National Level in 2001. In addition, Longhushan was also one of the birthplaces of Taoism, and its red cliffs and clear waters inspired many cultural thoughts of Taoism. Zhengyi Temple, the ancestral temple of Taoism, is located at the foot of Yunjin Peak (Figure 3h). Mazuyan, Nanyan Temple, Shuangyan Temple, and Jinlong Peak are historically renowned Buddhist sites. Xiangshan Academy, one of the four great academies during the Southern Song Dynasty, is located in the Yingtianshan Scenic Area (Figure 3i).

3. Data and Methods

3.1. Data Acquisition and Processing

The data required for this study were obtained from field surveys and secondary sources, with detailed information on the data sources provided in Table 1. The study was conducted during 2024–2026, encompassing field investigations, data collection, spatial analysis and manuscript preparation. All spatial analyses were conducted using ArcGIS 10.7 and ArcGIS Pro3.4.3 to facilitate data processing and spatial analysis.

Table 1. Data sources.

Data Type	Data Resolution	Data Sources
Geological map	1:100,000	Jiangxi Bureau of Geology and Mineral Resources
ASTER DEM	12.5 m	ALOS PALSAR dataset https://search.asf.alaska.edu (accessed on 9 June 2025)
Hydrological data	30 m	National Platform for Common GeoSpatial Information Service https://www.tianditu.gov.cn/
Soil type data	30 m	Soil Science Database https://vdb3.soil.csdb.cn
Land-use type data	30 m	National Platform for Common GeoSpatial Information Service https://www.tianditu.gov.cn/

3.2. Field Survey

The geodiversity characteristics of Longhushan UGGp were collected through field surveys and literature reviews. Based on these, eight representative assessment indicators were selected, including lithology, slope, and soil type, to construct an evaluation index system for the geodiversity of Longhushan UGGp (Table 2).

Table 2. Geodiversity evaluation system for Longhushan UGGp and indicator meanings.

Primary Indicator	Secondary Indicator	Meaning
Geology	Lithology	Bedrock of the landscape and landforms.
	Tectonic Fracture	Control factor for the spatial pattern and configuration of the landscape and the degree of landform fragmentation.
Geomorphology	Slope	Steepness of a surface and its influence on gravitational geomorphic processes, such as collapses.
	Relief Energy (RE)	Relative elevation difference and degree of terrain dissection, serving as an important indicator for classifying terrain types.
	Topographic Position Index (TPI)	Classification of different terrain positions, such as ridges, valleys, and gentle slopes.
Hydrology	Water Area	Development degree and spatial distribution of surface-water bodies.
Pedology	Soil Type	Relationship between parent material and surface processes.
	Land-Use Type	Degree of human intervention in geological processes and geographical environment.

3.3. Geodiversity Assessment

The quantitative evaluation method of geodiversity based on fishnet grids proposed by Pereira et al. [11] was adopted. This method discretizes the continuous geographical space into independent evaluation units by superimposing a grid array of fixed cell size over the study area. Based on the size of the major geomorphological units in the study area, we selected a 1 km × 1 km grid as the basic mapping unit. This resolution was chosen to effectively capture the spatial variation in geodiversity while avoiding excessive data redundancy and computational burden. A total of 1139 grid cells were generated. The subindex is obtained by counting the categories or quantities of each index within each grid cell. Then, the total geodiversity index was calculated by weighted overlay of the subindices. The total geodiversity index is expressed as

$$GI = G_g \times \omega_g + G_m \times \omega_m + G_h \times \omega_h + G_s \times \omega_s \quad (1)$$

where GI is the total geodiversity index, G_g is the geological index, G_m is the geomorphological index, G_h is the hydrological index, G_s is the soil index, and ω denotes the weight for each index. Following the method proposed by Jenks [39], each subindex and the total geodiversity index are classified into five categories: very low, low, medium, high, and very high.

The specific procedure for the geodiversity assessment is shown in Figure 4.

3.4. Principal Component Analysis (PCA)

To objectively reflect the contribution of each factor to the geodiversity assessment, the PCA method was adopted to determine the weights of each index. Since the evaluation indicators possess varying physical dimensions and numerical ranges, Z-score standardization was applied to the data to eliminate dimensional effects. The standardization was performed as

$$Z_{ij} = \frac{X_{ij} - \overline{X}_j}{\sigma_j} \quad (2)$$

where X_{ij} is the original value of the j-th indicator in the i-th grid cell, $\overline{X}_j$ is the mean of the j-th indicator, and σ_j is its standard deviation.

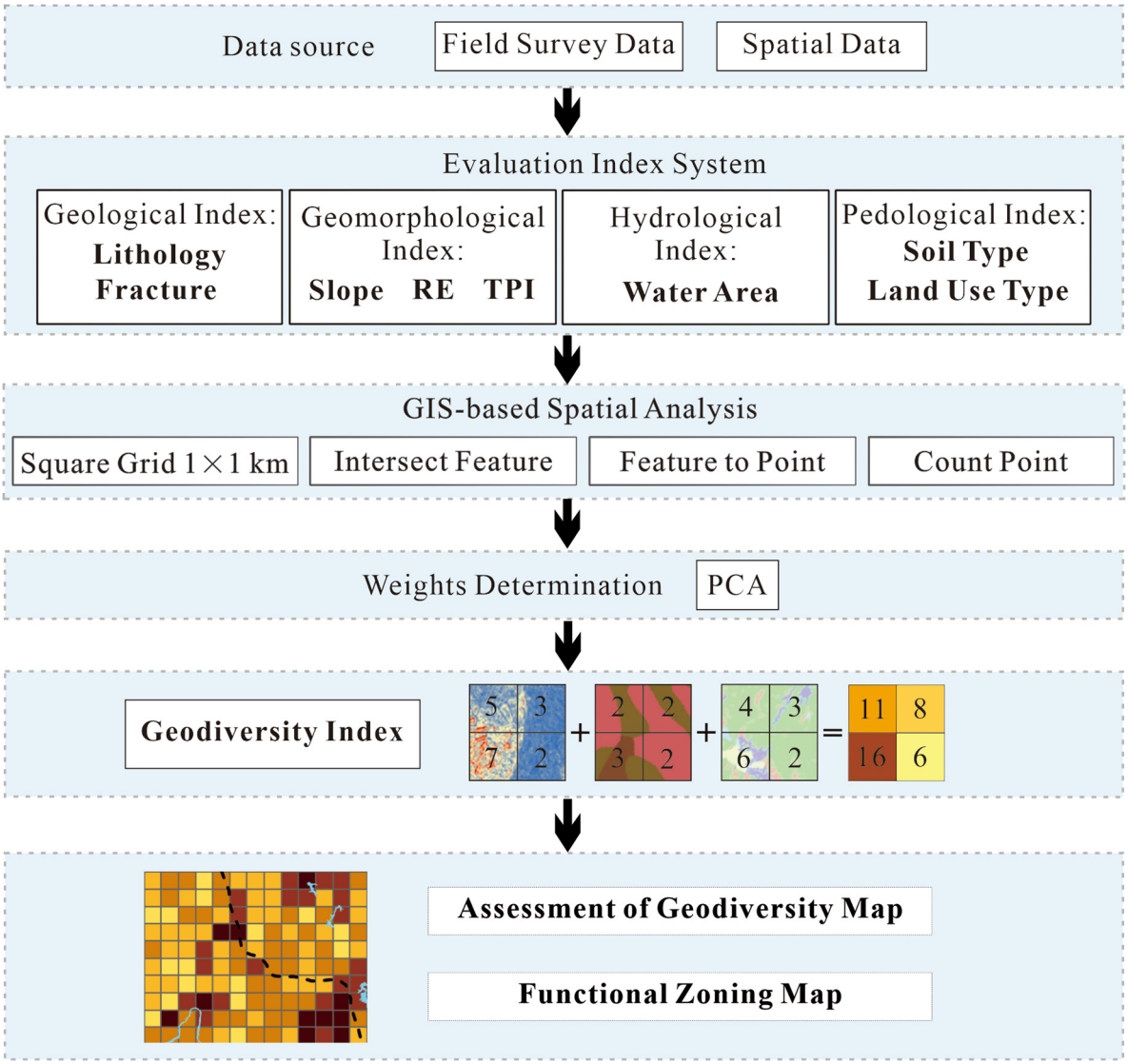


Figure 4. Flowchart of the key steps for quantitative geodiversity assessment in this study.

PCA was subsequently applied to the standardized values of the eight indicators across the 1139 grid cells. The Kaiser–Meyer–Olkin (KMO) measure of sampling adequacy and Bartlett's test of sphericity were calculated to verify the suitability of the data for PCA. Principal components with eigenvalues greater than 1 were retained following the Kaiser criterion. The cumulative variance contribution rate of the retained components was then calculated.

To derive the comprehensive weight for each indicator, the factor loadings of each indicator on the retained principal components were extracted from the component matrix. The weight of the j-th indicator was calculated as

$$\omega_j = \frac{\sum_{k=1}^{m} \left| L_{jk} \right| \times \lambda_k}{\sum_{j=1}^{n} \sum_{k=1}^{m} \left| L_{jk} \right| \times \lambda_k} \quad (3)$$

where ω_j is the weight of the j-th indicator, L_{jk} is the factor loading of the j-th indicator on the k-th retained principal component, λ_k is the eigenvalue of the k-th principal component, m is the number of retained principal components, and n is the number of indicators (n = 8).

This approach ensures that principal components with larger eigenvalues contribute more to the weight calculation, and indicators with higher loadings on these components receive greater weights. The resulting weights were then aggregated according to the four primary indicator categories to obtain the comprehensive weight for each primary indicator (Figure 5).

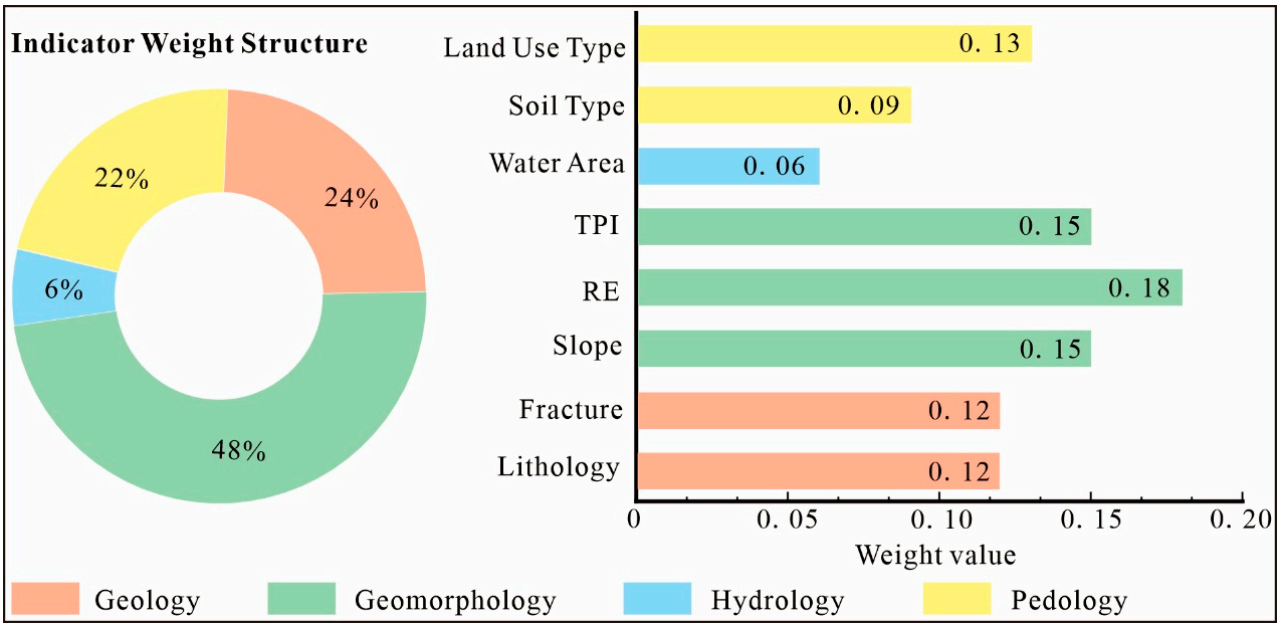


Figure 5. Weight distribution of the geodiversity assessment indicator system.

4. Geodiversity Assessment Results

4.1. Geology Index

According to the weighting scheme, the geology index receives a weight of 0.24, with lithology and fracture each accounting for 0.12 (Figure 5), indicating their equal influence on the overall geodiversity evaluation. As shown in Figure 6, high-value areas of fault and strata type counts are mainly concentrated in the Guifeng area in the northeastern part of the geopark and the Longhushan and Yingtianshan areas in the south, where fault structures are densely developed, and the Late Cretaceous red beds exhibit diverse lithological associations. In contrast, the vast central and northwestern regions are characterized by sparse faults and homogeneous bedrock lithology, resulting in generally low geological index values. Their lithological associations are dominated by conglomerates interbedded with sandstones, and this complex assemblage provides a pronounced material basis for differential weathering, which underpins the development of positive landforms such as cliffs and mesas. Tectonic fractures predominantly run in NE, NW, and nearly E-W directions, consistent with the regional principal tectonic lineaments [31].

4.2. Geomorphology Index

Among all primary indicators (Figure 5), the geomorphology index is assigned the largest weight (0.48). Its three subindicators, slope (0.15), RE (0.18) and TPI (0.15), collectively highlight the overriding control of topographic relief and landform diversity on geodiversity. The geomorphological diversity displays an overall spatial pattern of being high in the southeast and low in the northwest (Figure 7), dominated by low (70.94%) and

medium (16.07%) values. High-value areas account for a small proportion (13.26%) and are concentrated in core scenic zones such as Guifeng and Xianshuiyan in the east and Yingtianshan in the southwest. These high-value areas correspond to regions characterized by high relief amplitude, steep slope variations, and diverse landform types, closely matching the spatial distribution of typical geoheritage sites such as peak forests, peak clusters, cliffs, and gorges. Although high-value areas account for a limited proportion of the total area, they contribute substantially to the overall geomorphological diversity. They represent both the core scenic zones for geotourism development and the key areas for geoconservation.

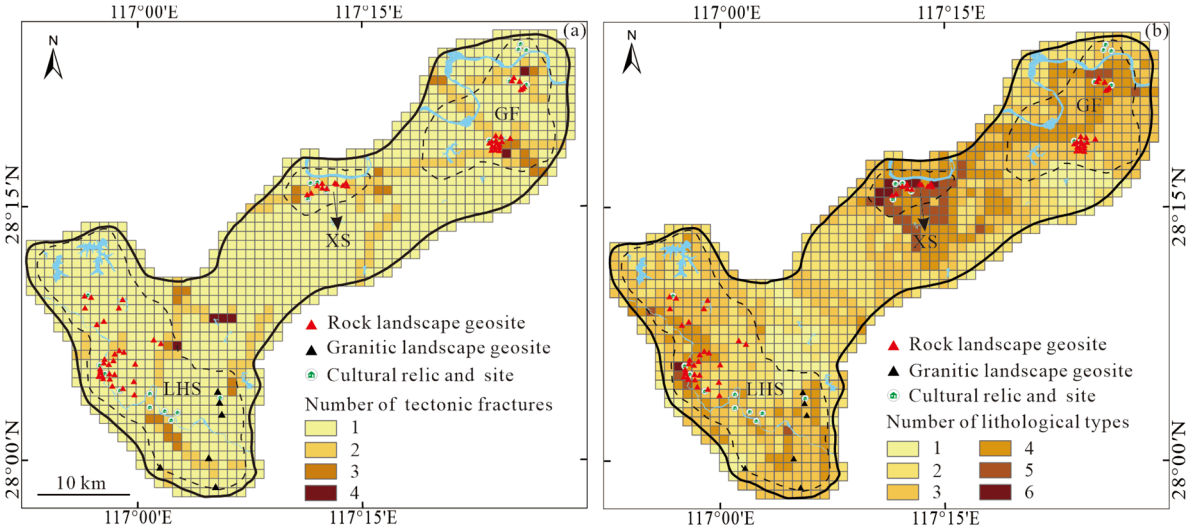


Figure 6. Geology subindex geodiversity map of Longhushan UGGp. (**a**) Number of tectonic fractures; (**b**) number of lithological types. The black dashed lines delineate the boundaries of the Longhushan (LHS), Xiangshan (XS), and Guifeng (GF) scenic areas, and the blue features delineate surface water.

4.3. Hydrology Index

In our assessment, the hydrology index has the lowest weight (0.06) among the four primary indicators (Figure 5), reflecting the relatively minor yet nonnegligible role of surface-water bodies in the study area. The spatial distribution of hydrological diversity in Longhushan UGGp displays a pronounced banded pattern extending along the drainage network (Figure 8). Low-value areas of hydrological diversity account for 91.92% of the geopark, covering most of its area and corresponding to terrestrial surfaces with sparse open water bodies. The medium-value (3.95%) and high-value (4.47%) areas are distributed as continuous bands along the main stream of the Xin River and the Luxi River. Although the high-value areas account for a limited proportion, they contribute significantly to the formation and evolution of landforms. Controlled by fault structures, rivers continuously reshape cliff morphology through ongoing downcutting and lateral erosion, promoting the retreat of steep cliffs and the deepening of gorges, thus serving as a key driving force in the formation and evolution of erosional landscapes.

4.4. Pedology Index

With a weight of 0.22 (Figure 5), the pedology index ranks second among the primary indicators. Its two subindicators, soil type (0.09) and land-use type (0.13), capture the combined effects of surface cover and anthropogenic disturbance on geodiversity. Spatially, areas with a greater variety of soil types are concentrated mainly in the central and northeastern parts (Figure 9a), where the terrain is relatively flat, favoring the accumulation and preservation of soil parent materials such as fluvial deposits and weathered

residues from red beds. Combined with favorable hydrothermal conditions, a variety of soil types have developed, including red soils, yellow soils, and paddy soils. In the central and northeastern parts, where soil types are more diverse, particularly near settlements, along riverbanks, and on the surrounding alluvial plains, human activities exert a strong influence. Land use is dominated by cropland, forest land, and built-up areas, showing a relatively high diversity (Figure 9b).

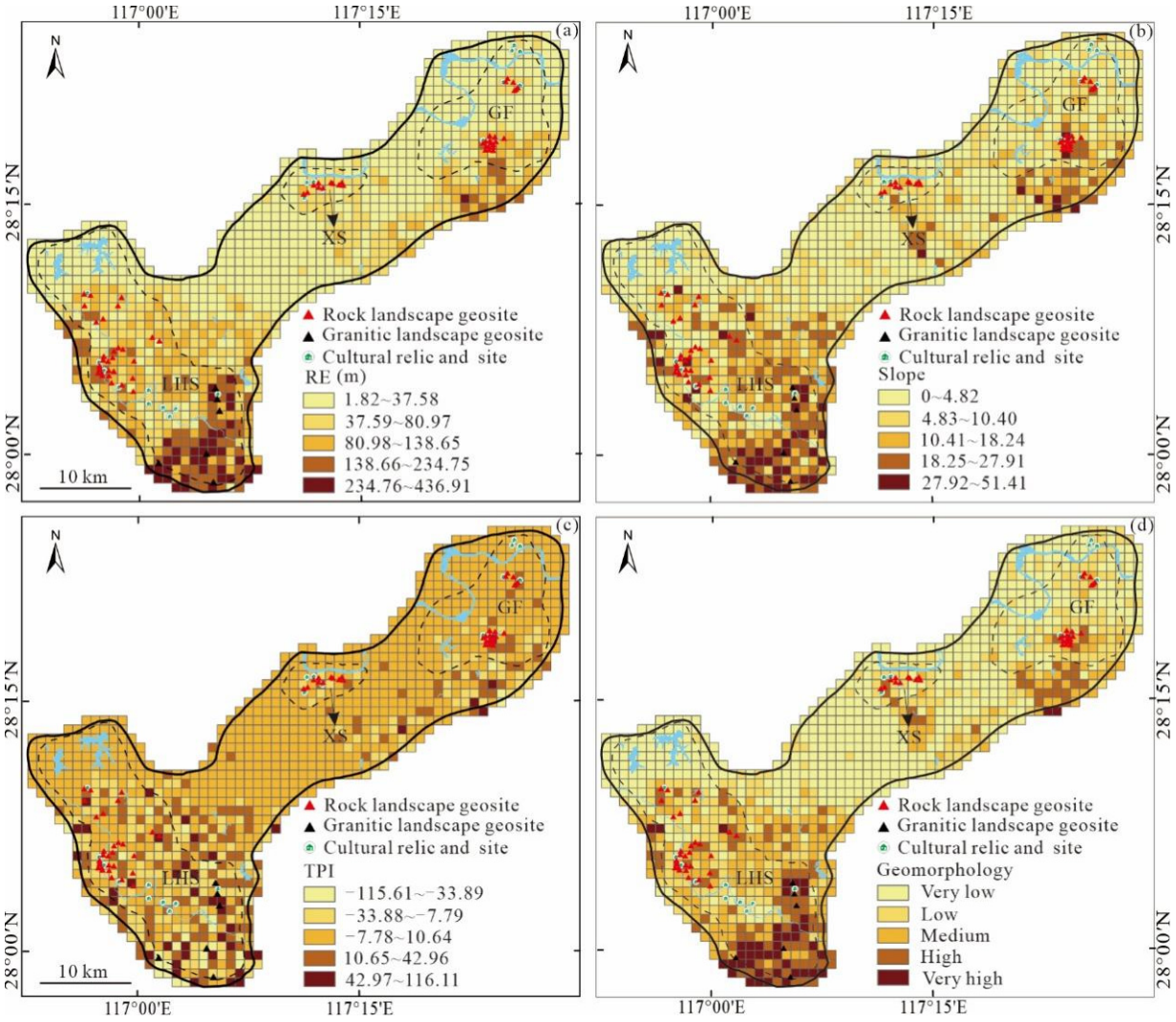


Figure 7. Geomorphic geodiversity subindex map of Longhushan UGGp. (**a**) relief energy (RE); (**b**) represent slope; (**c**) topographic position index (TPI); (**d**) geomorphological geodiversity subindex. The black dashed lines delineate the boundaries of the Longhushan (LHS), Xiangshan (XS), and Guifeng (GF) scenic areas, and the blue features delineate surface water.

4.5. Total Geodiversity Index

Based on the eight geodiversity factors described above, the weight of each factor was determined using PCA. The geodiversity index of Longhushan UGGp was then calculated and visualized to produce a total geodiversity map (Figure 10). The natural breaks method [39] was applied to classify the total into five GI levels: very high, high, medium, low, and very low. The total geodiversity map exhibits significant spatial heterogeneity, with very high values mainly concentrated in the southwest, moderate-to-high values in the northeast, and low values in the central and northwestern areas.

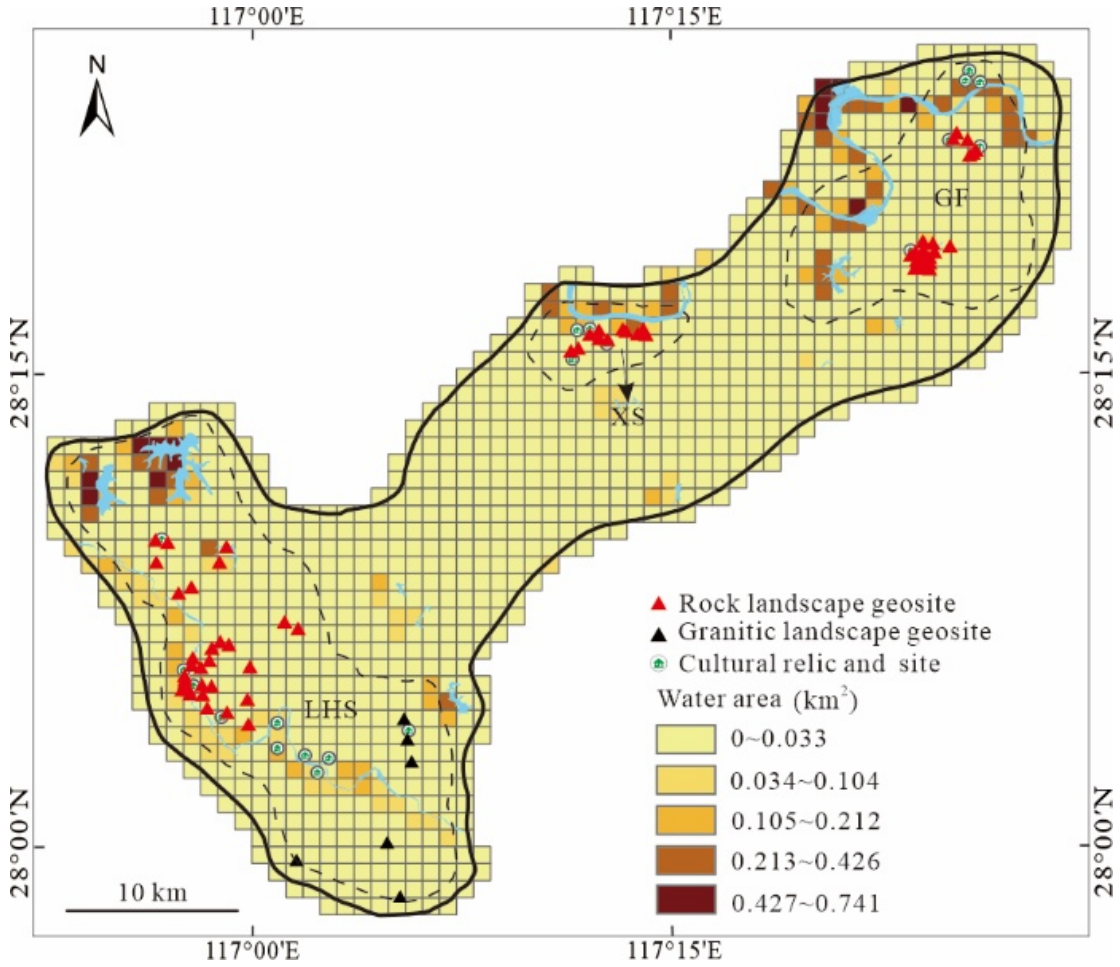


Figure 8. Hydrology subindex geodiversity map of Longhushan UGGp. The black dashed lines delineate the boundaries of the Longhushan (LHS), Xiangshan (XS), and Guifeng (GF) scenic areas, and the blue features delineate surface water.

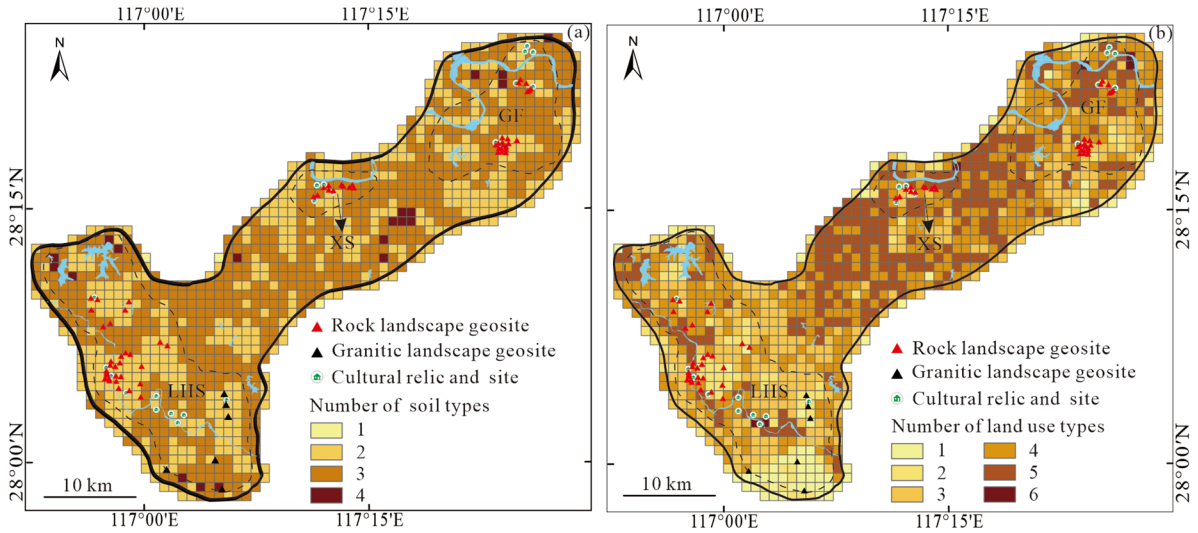


Figure 9. Pedology subindex geodiversity map of Longhushan UGGp. (**a**) Number of soil types; (**b**) number of land-use types. The black dashed lines delineate the boundaries of the Longhushan (LHS), Xiangshan (XS), and Guifeng (GF) scenic areas, and the blue features delineate surface water.

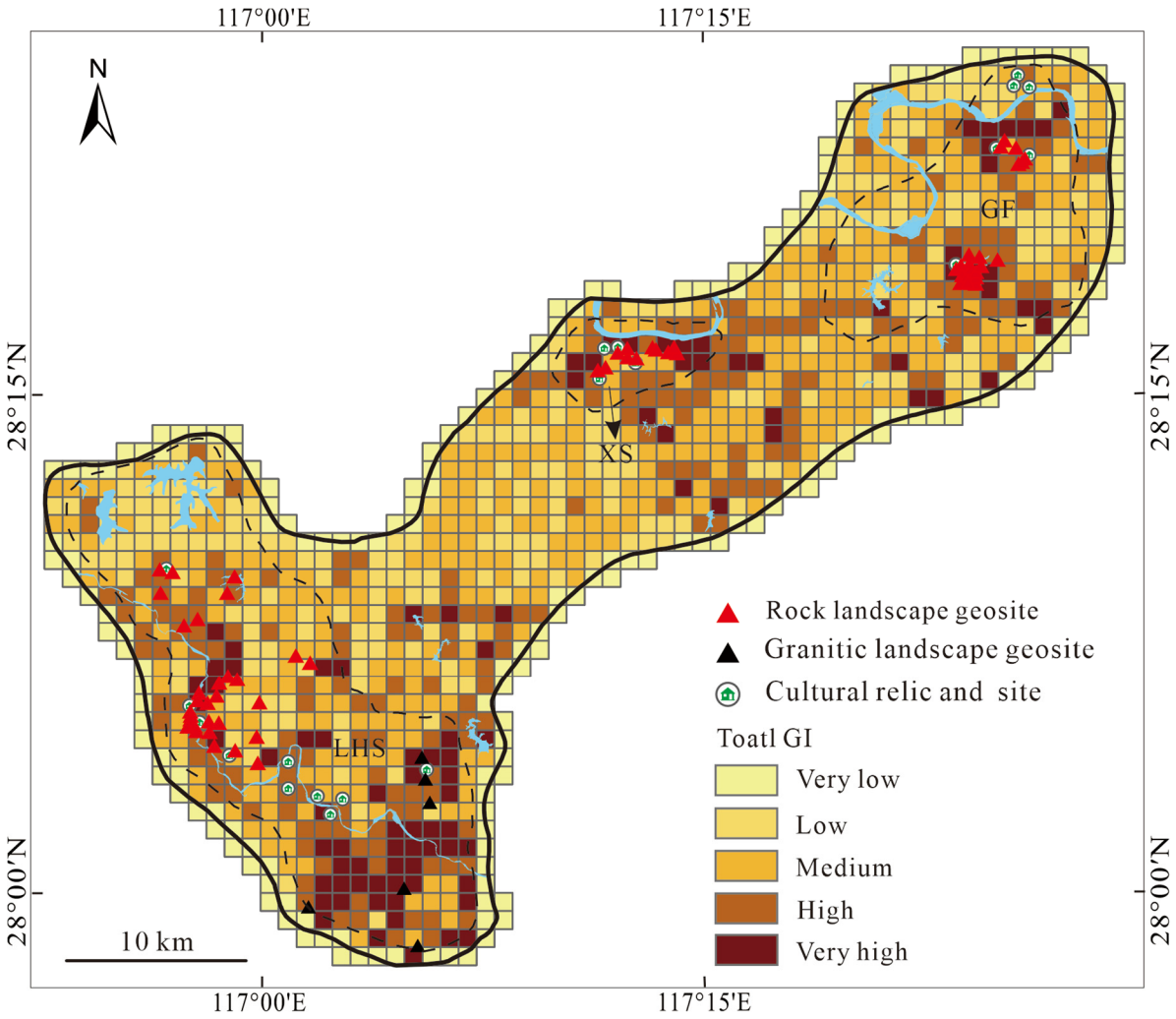


Figure 10. Total geodiversity map of Longhushan UGGp. The black dashed lines delineate the boundaries of the Longhushan (LHS), Xiangshan (XS), and Guifeng (GF) scenic areas, and the blue features delineate surface water.

Areas with very high geodiversity values account for 6.67% of the total area (Table 3) and are mainly concentrated in the Guifeng, Xiangshan, Longhushan and Yingtianshan areas. Areas with high geodiversity values account for 15.63% (Table 3). They show a broader but discontinuous distribution. In the Longhushan area, high GI levels are concentrated mainly in the south and southwest. They are also distributed in the east of the geopark, particularly in Xiangshan and the center and south of Guifeng.

Table 3. Percentages of the area of Longhushan UGGp representing specific levels of geodiversity.

GI Level	Geodiversity Factor (%)				Total GI (%)
	Geology	Geomorphology	Hydrology	Pedology	
Very low	37.31	47.15	86.48	11.15	26.08
Low	46.97	23.79	5.44	14.14	24.14
Medium	11.94	16.07	3.95	26.51	27.48
High	3.33	9.22	3.25	30.20	15.63
Very high	0.43	4.04	1.23	18.01	6.67

The medium geodiversity value areas are the most widely distributed type in the geopark, accounting for 27.48% (Table 3). They are widely distributed across the central and

northeastern parts, mainly corresponding to low-relief residual hills and floodplains. In these zones, the red sandstones and conglomerates are progressively covered by Quaternary sediments, resulting in gentle landforms that display a transitional character from typical rugged terrains to ordinary landforms.

The low and very low geodiversity areas account for 24.14% and 26.08% of the total area. They are mainly distributed in the central parts and plains of the geopark, where they feature a homogeneous lithology, primarily consisting of Quaternary deposits, with low topographic relief, and land use dominated by cropland.

4.6. Functional Zoning

The spatial pattern of the total geodiversity index is used to delineate three functional zones within Longhushan UGGp: (1) the core conservation and utilization zone, (2) the key conservation and utilization zone, and (3) the ecological conservation buffer zone (Figure 11). These zones show clear spatial differentiation and generally correspond to different levels of geodiversity.

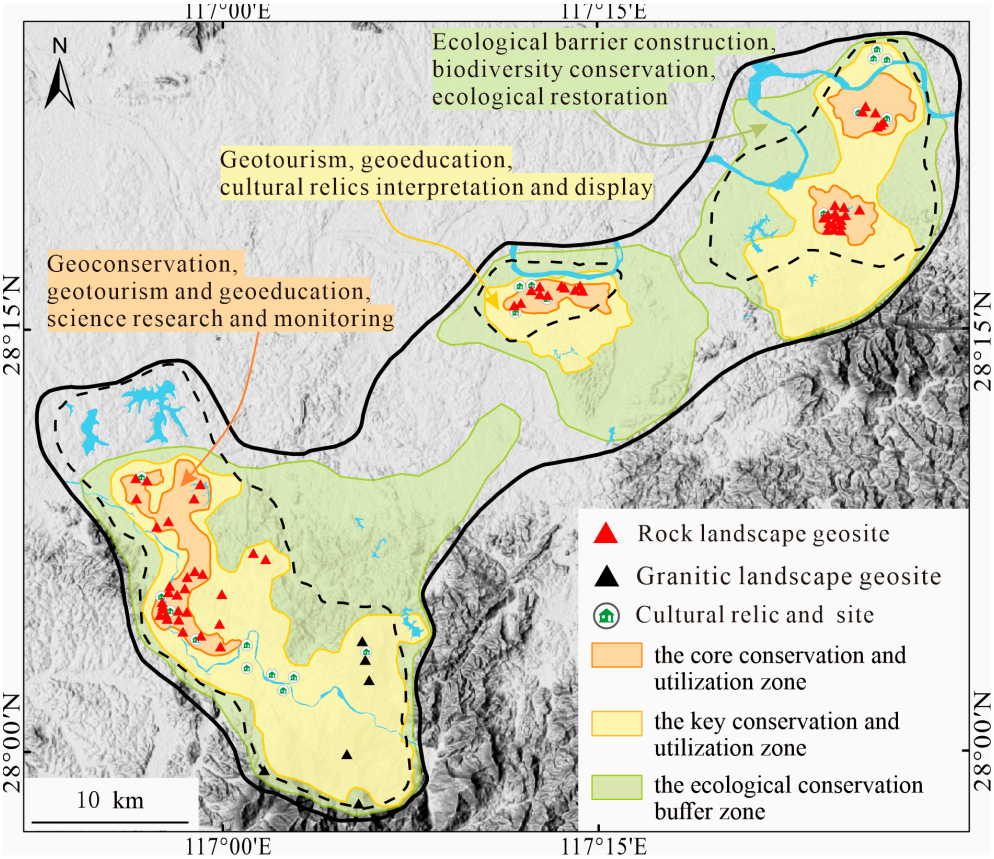


Figure 11. Functional zoning map based on total geodiversity assessment of Longhushan UGGp. The black dashed lines delineate the boundaries of the Longhushan (LHS), Xiangshan (XS), and Guifeng (GF) scenic areas, and the blue features delineate surface water.

The core conservation and utilization zones are mainly concentrated in Xianshuiyan, Xiangshan, Guifeng, and Yingtianshan, corresponding largely to areas of high and very high geodiversity. These zones show relatively concentrated distributions and encompass the major areas with complex geological and geomorphological features. The key conservation and utilization zones are mainly distributed around the core zones and in areas with moderate geodiversity, forming transitional belts between the core and surrounding areas. In contrast, the ecological conservation buffer zones are mainly located in the central and

northwestern parts and along the peripheral areas of the geopark, where low and very low GI values predominate.

5. Discussion

5.1. Spatial Heterogeneity and Controls of Geodiversity

Longhushan UGGp exhibits pronounced spatial heterogeneity in geodiversity, with high GI areas concentrated mainly in Xianshuiyan, Xiangshan, Guifeng, and Yingtianshan, whereas lower values occur predominantly in the central and northwestern parts of the geopark. These high GI areas broadly coincide with the distribution of representative geoheritage features, including peak forests, cliffs, pillars, arches, and gorges. Because geosites were not included as indicators in the GI calculation, this spatial correspondence suggests that the assessment effectively identifies areas where geological and geomorphological diversity is concentrated, rather than simply reproducing the distribution of recognized geosites. Similar associations between high geodiversity and important geoheritage have also been reported in previous studies [17,23]. These findings further support the potential of geodiversity assessment as a complementary tool for identifying areas of high geoheritage and conservation value.

The spatial pattern of geodiversity is most strongly associated with topographic differentiation, together with lithological and tectonic fractures. Among the eight indicators, relief energy (RE) received the highest weight (0.18), followed by slope (0.15) and TPI (0.15), highlighting the importance of terrain relief and topographic position in shaping the present geodiversity pattern. The prominence of these terrain-related indicators has a clear geomorphological basis. Hjort and Luoto [40], for example, found that areas of high geodiversity in northern Finland were preferentially associated with steep-sided valleys, where heterogeneous terrain supports the coexistence of multiple erosional and depositional processes. It should nevertheless be noted that the PCA-derived weights in the present study represent the relative statistical contributions of individual indicators to the composite GI and should not be interpreted directly as measures of geomorphic causality. Areas with greater relief and slope variation generally support a wider range of erosional landforms, while lithological differences and fracture systems provide the material and structural conditions for differential weathering, rock dissection, and erosion. This interpretation is consistent with the geological setting of Longhushan, where faults and joints promote preferential fluvial erosion and the development of characteristic Danxia landforms [30]. Thus, the spatial pattern of geodiversity likely results from the combined effects of topography, lithology, geological structure, and erosion.

Although hydrology received the lowest PCA-derived weight (0.06), this should not be interpreted as indicating limited importance for landscape evolution and conservation. In this study, hydrology is represented by surface-water area, whereas long-term fluvial incision and lateral erosion remain important processes shaping cliffs, gorges, and other erosional landforms. Therefore, hydrological conditions and associated fluvial erosion should be considered in the long-term monitoring of the geopark, particularly in areas where important geoheritage is closely related to river incision. Such monitoring would help identify potential changes that may affect the stability and preservation of these landforms.

5.2. Scientific and Management Implications of Functional Zoning

Quantitative geodiversity assessment provides a spatial basis for distinguishing areas with different conservation and land-use priorities. Previous studies have shown that geodiversity mapping can support the identification of priority areas and contribute to land-use planning and protected-area management [4,27]. Quantitative assessment can also provide a useful basis for establishing conservation and management priorities [41].

In Longhushan UGGp, functional zoning further translates the spatial differences revealed by the GI into differentiated conservation and utilization strategies. Areas with high geodiversity and concentrated geoheritage require stronger protection of landform integrity and geological features, whereas areas with moderate geodiversity can accommodate controlled geotourism and geoeducation under appropriate conservation measures [42]. Lower GI areas should not be regarded as having little value; rather, they can serve as buffer spaces that help reduce development pressure on high GI areas. This differentiated approach is consistent with the broader principle that geodiversity and geoheritage should be integrated into protected-area planning and management.

The zoning also provides a practical basis for matching management intensity to landscape conditions. In the core zones, priority should be given to maintaining the integrity of representative geosites and controlling intensive construction or tourism disturbance; in the key zones, conservation can be combined with appropriately regulated tourism and educational use; and the buffer zones can help mitigate external disturbance and maintain the environmental setting of the geopark. Such spatial differentiation is particularly relevant in Longhushan, where many representative rock landscapes occur in areas of relatively steep and dissected terrain. Recent research has also emphasized the ecological sensitivity of steeply sloping land and the need for stronger monitoring and control where development pressures increase [43]. However, GI alone should not be regarded as the sole basis for management decisions; potential threats, tourism pressure, and landscape vulnerability should also be considered [44]. Therefore, the proposed zoning is not simply a classification of GI values but a spatial decision tool for targeted conservation and sustainable land-use management.

6. Conclusions

The geodiversity of Longhushan UGGp exhibits pronounced spatial heterogeneity, with high values in the southwest and northeast and lower values in the central and northwestern parts. Specifically, areas with very high and high values together account for 22.30% of the geopark, concentrated mainly in the Xianshuiyan, Xiangshan, Guifeng, and Yingtianshan regions. In contrast, areas with low and very low values cover 50.22%, occurring predominantly on the floodplains along the Xin River and in the peripheral zones of the geopark.

The assessment identified geodiversity hotspots that closely coincide with representative geoheritage features, particularly erosional rock landforms developed on a reddish conglomerate-dominated succession through the interplay of fracture systems, fluvial erosion, weathering, and mass collapse.

Based on these results, three functional zones were delineated: core conservation and utilization zone, key conservation and utilization zone, and ecological conservation buffer zone. This zoning scheme provides a practical basis for geoconservation, geotourism development, and the planning and management of Longhushan UGGp. Moreover, the assessment approach and functional zoning framework presented here can serve as a reference for the geoconservation and sustainable development of Southeast China, which is characterized by similar rock landscapes.

Author Contributions: Conceptualization, L.C. and H.L.; methodology, H.L.; software, H.L.; formal analysis, H.L.; investigation, L.C., B.L. and H.L.; data curation, H.L.; writing—original draft preparation, H.L.; writing—review and editing, L.C., Y.N. and B.L.; funding acquisition, L.C. All authors have read and agreed to the published version of the manuscript.

Funding: This research was funded by the National Natural Science Foundation of China, grant number 42361002; the Innovation Fund for Graduate Students of East China University of Technology,

grant number DHYC-2025005; and the Scientific Research Development Fund of East China University of Technology, grant numbers K20240018 and FZJJ20231220.

Data Availability Statement: The ASTER DEM data were obtained from the ALOS PALSAR dataset (https://search.asf.alaska.edu (accessed on 9 June 2025)). Hydrological and land use data were sourced from the National Platform for Common GeoSpatial Information Service (https://www.tianditu.gov.cn/). Soil type data were acquired from the Soil Science Database (https://vdb3.soil.csdb.cn). Field survey data supporting the findings of this study are available from the corresponding author upon reasonable request.

Acknowledgments: The authors acknowledge the Longhushan Scenic Area Administrative Committee of Yingtan City for supporting field investigations. We also thank the editors and anonymous reviewers for their constructive comments that helped improve this manuscript.

Conflicts of Interest: The authors declare no conflicts of interest. The funders had no role in the design of the study; in the collection, analyses, or interpretation of data; in the writing of the manuscript; or in the decision to publish the results.

References

1. Serrano, E.; Ruiz-Flaño, P. Geodiversity: A theoretical and applied concept. *Geogr. Helv.* **2007**, *62*, 140–147. [CrossRef]
2. Crisp, J.R.A.; Ellison, J.C.; Fischer, A. Current trends and future directions in quantitative geodiversity assessment. *Prog. Phys. Geogr. Earth Environ.* **2021**, *45*, 514–540. [CrossRef]
3. Queiroz, L.S.; Diniz, M.T.M.; de Medeiros, J.F.; Brandão, A.; Xavier, R.A. Geodiversity, Pareidolia and Geomythology: A Cultural Reading of Granite Rocks in Brazil's Northeast Region. *Geoheritage* **2025**, *17*, 152. [CrossRef]
4. Quintero-Marín, J.E.; Rendón-Rivera, A.; Brilha, J. A Study on Geodiversity and Geoconservation's Impact on the Management of Natural Resources in the Alto Ricaurte Region, Boyacá, Colombia. *Geoheritage* **2023**, *15*, 122. [CrossRef]
5. Anougmar, S.; Meesters, A.; Van Ree, D.; Compernolle, T. The dilemma of valuing geodiversity: Geoconservation versus geotourism. *Philos. Trans. R. Soc. A* **2024**, *382*, 20230049. [CrossRef] [PubMed]
6. Yahya Sheibani, V.; Zamanian, E. Geodiversity and Geological Treasure of Tabas UNESCO Global Geopark for Geotourism Development, New UGGp from Iran. *Geoheritage* **2023**, *15*, 106. [CrossRef]
7. Adrianda, R.S.; Sahara, R.; Gusti, U.K. The geodiversity site of Geopark Ranah Minang Silokek, Indonesia: Promoting geo-education and geotourism through geosite assessment. *Int. J. Geoheritage Parks* **2025**, *13*, 239–249. [CrossRef]
8. Scammacca, O.; Bétard, F.; Aertgeerts, G.; Heuret, A.; Fermet-Quinet, N.; Montagne, D. Geodiversity Assessment of French Guiana: Challenges and Implications for Sustainable Land Planning. *Geoheritage* **2022**, *14*, 83. [CrossRef]
9. Datta, K. Does geodiversity correlate with land use/land cover diversity? A case study of Birbhum district, West Bengal, India. *Proc. Geol. Assoc.* **2022**, *133*, 589–602. [CrossRef]
10. Tukiainen, H.; Alahuhta, J.; Field, R.; Ala-Hulkko, T.; Lampinen, R.; Hjort, J. Spatial relationship between biodiversity and geodiversity across a gradient of land-use intensity in high-latitude landscapes. *Landsc. Ecol.* **2017**, *32*, 1049–1063. [CrossRef]
11. Pereira, D.I.; Pereira, P.; Brilha, J.; Santos, L. Geodiversity Assessment of Paraná State (Brazil): An Innovative Approach. *Environ. Manag.* **2013**, *52*, 541–552. [CrossRef] [PubMed]
12. Zakharovskyi, V.; Németh, K. Quantitative-qualitative method for quick assessment of geodiversity. *Land* **2021**, *10*, 946. [CrossRef]
13. Wilhelm, M.; Zaghetti, A.F.G.; Weiss, R. Geodiversity and Landscape Structure in the Quarta Colônia UNESCO Global Geopark, Brazil: Compositional Richness and Land-Use and Land-Cover Fragmentation. *Soc. Nat.* **2026**, *38*, e81193. [CrossRef]
14. Brilha, J.; Gray, M.; Pereira, D.I.; Pereira, P. Geodiversity: An integrative review as a contribution to the sustainable management of the whole of nature. *Environ. Sci. Policy* **2018**, *86*, 19–28. [CrossRef]
15. Zwoliński, Z.; Najwer, A.; Giardino, M. Chapter 2—Methods for Assessing Geodiversity. In *Geoheritage*; Reynard, E., Brilha, J., Eds.; Elsevier: Amsterdam, The Netherlands, 2021; pp. 27–52. [CrossRef]
16. Szadkowska, K.; Szadkowski, M.; Tarka, R. Inventory and Assessment of the Geoheritage of the Sudetic Foreland Geopark (South-Western Poland). *Geoheritage* **2022**, *14*, 24. [CrossRef]
17. Ferrando, A.; Faccini, F.; Paliaga, G.; Coratza, P. A Quantitative GIS and AHP Based Analysis for Geodiversity Assessment and Mapping. *Sustainability* **2021**, *13*, 10376. [CrossRef]
18. dos Santos, D.S.; Mansur, K.L.; de Araújo, J.C.; de Souza Santos, E.E.; Ferreira, N.N. The importance of the subindices on quantitative assessment of geodiversity: A methodological discussion and application to the Geopark Costões e Lagunas, SE Brazil. *Environ. Earth Sci.* **2025**, *84*, 288. [CrossRef]
19. de Paula Silva, J.; Alves, G.B.; Ross, J.L.S.; de Oliveira, F.S.; do Nascimento, M.A.L.; Felini, M.G.; Manosso, F.C.; Pereira, D.Í. The Geodiversity of Brazil: Quantification, Distribution, and Implications for Conservation Areas. *Geoheritage* **2021**, *13*, 75. [CrossRef]

20. Alberico, I.; Casaburi, A.; Matano, F. Mapping Geodiversity at a National Scale: The Case Study of Italy. *Geoheritage* **2023**, *15*, 121. [CrossRef]
21. Coronato, A.; Schwarz, S. Approaching geodiversity and geoconservation in Argentina. *Int. J. Geoheritage Parks* **2022**, *10*, 597–615. [CrossRef]
22. Esmaili, R. Quantitative Evaluation and Spatial Clustering of Geodiversity in Iran. *Geoheritage* **2024**, *16*, 13. [CrossRef]
23. Carrión-Mero, P.; Dueñas-Tovar, J.; Jaya-Montalvo, M.; Berrezueta, E.; Jiménez-Orellana, N. Geodiversity assessment to regional scale: Ecuador as a case study. *Environ. Sci. Policy* **2022**, *136*, 167–186. [CrossRef]
24. Gakou, M.; Souhil, T.; Barragan-Jason, G.; Feuillet, T.; Bétard, F.; Cauchoix, M. Unveiling the spatial link between geodiversity and biodiversity: A multi-taxon study in the South of France. *Landsc. Ecol.* **2026**, *41*, 81. [CrossRef]
25. Tukiainen, H.; Maliniemi, T.; Brilha, J.; Alahuhtaet, J.; Hjort, J. A framework for quantifying geodiversity at the local scale: A case study from the Rokua UNESCO Global Geopark. *Philos. Trans. R. Soc. A* **2024**, *382*, 20230059. [CrossRef] [PubMed]
26. Zhang, Z.T.; Chen, L.Q.; Ng, Y.; Guo, F.S.; Liu, X. Characterization and Quantitative Assessment of Geodiversity in Danxiashan UNESCO Global Geopark of China. *Geoheritage* **2024**, *16*, 139. [CrossRef]
27. Xu, B.Y.; Yang, J.F.; Yu, Y.; Han, Y.S.; Wang, R.L. Spatial Patterns of Geodiversity and Their Relevance to Land Management in Mount Cangshan Global Geopark. *Land* **2026**, *15*, 223. [CrossRef]
28. Migoń, P. Geomorphology of conglomerate terrains–Global overview. *Earth Sci. Rev.* **2020**, *208*, 103302. [CrossRef]
29. Yi, J.; Chen, L.Q.; Ng, Y.; Chen, F. Red Beds Geoheritage in China and Australia: A Comparative Study between the Landscapes of Danxiashan UGGp and Purnululu National Park. *Geoheritage* **2026**, *18*, 97. [CrossRef]
30. Kusky, T.M.; Ye, M.; Wang, J.; Wang, L. Geological evolution of Longhushan World Geopark in relation to global tectonics. *J. Earth Sci.* **2010**, *21*, 1–18. [CrossRef]
31. Jiang, Y.B.; Guo, F.S.; Li, G.R.; Li, R.; Lou, F.S.; Wang, Z.; Chen, L.Q.; Qie, H.M.; Yan, L.B.; Li, Y.Z.; et al. Study on the evolution of Danxia landform in Jiangxi Province and its structural factors. *Geol. Rev.* **2024**, *1*, 44–58. (In Chinese with English Abstract) [CrossRef]
32. Chen, L.Q.; Guo, F.S.; Shao, C.J.; Lou, F.S.; Li, B.; Li, G.R.; Qie, H.M.; Wu, Z.Y.; Jiang, Y.B.; Liu, F.J. Characteristics and controlling factors of danxia landscapes in Jiangxi Province. *Acta. Geol. Sin.* **2022**, *96*, 4023–4037. (In Chinese with English Abstract) [CrossRef]
33. Chen, L.Q.; Guo, F.S. Upper Cretaceous alluvial fan deposits in the Jianglangshan Geopark of Southeast China: Implications for bedrock control on Danxia landform evolution. *J. Mt. Sci.* **2017**, *14*, 926–935. [CrossRef]
34. Guo, F.S.; Chen, L.Q.; Xu, H.; Liu, X. Origin of beaded tafoni in cliffs of Danxia landscapes, Longhushan Global Geopark, South China. *J. Mt. Sci.* **2018**, *15*, 2398–2408. [CrossRef]
35. Shu, L.S.; Zhou, X.M.; Deng, P.; Wang, B.; Jiang, S.Y.; Yu, J.H.; Zhao, X.X. Mesozoic tectonic evolution of the southeast China block: New insights from basin analysis. *J. Asian Earth Sci.* **2009**, *34*, 376–391. [CrossRef]
36. JBGMR (Jiangxi Bureau of Geology and Mineral Resources). *The Regional Geology of China: Jiangxi Monograph*; Geological Publishing House: Beijing, China, 2017; ISBN 978-7-116-10510-2.
37. Chen, L.Q.; Guo, F.S.; Steel, R.J.; Li, Y. Petrography and geochemistry of the Late Cretaceous redbeds in the Gan-Hang Belt, southeast China: Implications for provenance, source weathering, and tectonic setting. *Int. Geol. Rev.* **2016**, *58*, 1196–1214. [CrossRef]
38. Guo, F.S.; Jiang, Y.B.; Liu, L.Q.; Li, H. Evolution and Genesis System Features of Danxia Landform in Longhushan World Geopark. *J. Mt. Sci.* **2011**, *29*, 195–201. (In Chinese with English Abstract) [CrossRef]
39. Jenks, G.F. The Data Model Concept in Statistical Mapping. In *International Yearbook of Cartography*; C. Bertelsmann Verlag: Gütersloh, Germany, 1967; Volume 7, pp. 186–190, *in press*.
40. Hjort, J.; Luoto, M. Geodiversity of high-latitude landscapes in northern Finland. *Geomorphology* **2010**, *115*, 109–116. [CrossRef]
41. Brilha, J. Inventory and Quantitative Assessment of Geosites and Geodiversity Sites: A Review. *Geoheritage* **2016**, *8*, 119–134. [CrossRef]
42. Ferdowsi, S.; Tavana, M.; Heydari, R.; Strba, L. Geoeducation: The key to geoheritage conservation in tourism destinations. *Int. Geol. Rev.* **2025**, *67*, 1674–1696. [CrossRef]
43. Zhang, H.; Chai, J.; Li, Z.; Li, H.; Gibson, J.; Kumar, P.; Jin, G. Global effects of progress towards SDGs on steeply sloped land use and land cover. *Fundam. Res.* 2025, *in press*. [CrossRef]
44. Babicová, Z.; Molokáč, M.; Pachinger, P.; Molitoris, L. Management of geosites in geoparks based on the quantitative and potencial threats assessment: Example of the emerging Zemplín Geopark. *Geoheritage* **2026**, *18*, 50. [CrossRef]

Disclaimer/Publisher's Note: The statements, opinions and data contained in all publications are solely those of the individual author(s) and contributor(s) and not of MDPI and/or the editor(s). MDPI and/or the editor(s) disclaim responsibility for any injury to people or property resulting from any ideas, methods, instructions or products referred to in the content.